JOURNAL OF THE PHYSICAL SOCIETY OF JAPAN, Vol. 42, No. 3, MARCH

Dielectric Properties of Rubidium Nitrate under Hydrostatic Pressure

Sanji FUJIMOTO, Naohiko YASUDA, Hiroyasu SHIMIZU, Shigemi TSUBOI, Kazuo KAWABE,† Yutaka TAKAGI†† and Michio MIDORIKAWA††

Electrical Engineering Department, Gifu University, Kagamigahara, Gifu
†*Electrical Engineering Department, Osaka University, Suita, Osaka*
††*Synthetic Crystal Research Laboratory, Faculty of Engineering, Nagoya University, Nagoya*

(Received September 3, 1976)

The relative permittivity (ε_r) and dielectric conductivity (σ) of $RbNO_3$ single crystals were measured at 1 MHz under hydrostatic pressures over its two phase transformations; II-III (219 °C at 1 atm) and III-IV (164 °C at 1 atm). The value of ε_r has a large peak at the II-III phase transition pressure, and $1/\varepsilon_r$ obeys the Curie-Weiss law on pressure in the phase III. This behavior of ε_r is elucidated by the phenomenological theory for the first order antiferroelectric phase transition. The II-III phase boundary was determined by the dielectric measurement. At the IV-III phase transition temperature (T_c), the changes in ε_r and σ seen in the ε_r vs. T and σ vs. T curves get smaller with increasing applied-pressure. The behavior of ε_r and σ is explained by taking account of the rotation of NO_3^- ions being hindered by the pressure.

§1. Introduction

The physical properties of rubidium nitrate ($RbNO_3$) have been investigated by various techniques, i.e., X-ray diffraction and differential thermal analysis methods and dilatometric, electric and infrared-spectroscopic measurements, etc., and it was established that $RbNO_3$ has four stable forms between room temperature and the melting point under atmospheric pressure:[1]

$$\underset{\text{trigonal}}{\text{IV}} \overset{164\,^\circ\text{C}}{\cdots\cdots} \underset{\text{cubic}}{\text{III}} \overset{219\,^\circ\text{C}}{\cdots\cdots} \underset{\text{rhombohedral}}{\text{II}} \overset{285\,^\circ\text{C}}{\cdots\cdots} \underset{\text{cubic}}{\text{I}} .$$

While ordinary crystals have higher symmetry in the higher temperature phase, the $RbNO_3$ crystal has higher symmetry in the lower temperature phase for the III-II phase transition. Thus, the phase transition of $RbNO_3$ at the III-II transition point is similar to that of ferroelectric Rochelle salt at the lower Curie point.[2]

For the III-II phase transition, Dantsiger and Fesenko[3] pointed out that this transition is the antiferroelectric phase transition from the paraelectric phase to the antiferroelectric one on the basis of the following experimental results; (1) the permittivity has a peak at the transition point, (2) the reciprocal permittivity varies linearly with temperature near the transition point and (3) the permittivity increases with increasing dc electric field in the phase II.

For the phase IV, Bury and McLaren[4] reported from pyroelectric and optical measurements, direct observation of domains and X-ray diffraction methods that $RbNO_3$ belongs to the space group $P3_1$ (or $P3_2$) and the spontaneous polarization exists in the direction of the trigonal axis (c-axis). But no hysteresis loop was seen by oscilloscope examination.[3] Thus it is not clear whether the phase IV is ferroelectric or not.

Moreover Salhotra *et al.*[5] measured the dielectric conductivity (σ) versus temperature at all the four phase transformations and explained the behavior of σ in terms of crystal structures of $RbNO_3$, mainly on the basis of the rotation of NO_3^- ions.

On the other hand, the pressure study of $RbNO_3$ was done on its III-IV phase transition by Bridgman[6] and on the melting curve (III-Liquid phase transition) by Owens,[7] by means of the volume discontinuity method. However, any available high pressure study on the I-II and the II-III phase transition has not

been presented.

In this paper, we present the pressure dependence of permittivity and dielectric conductivity for the II-III and III-IV phase transitions of $RbNO_3$, and try to elucidate such a behavior by the aid of the phenomenological theory and terms of crystal structures.

§2. Preparation of Sample and Experimental Method

The $RbNO_3$ single crystals were grown by using slow evaporation method at room temperature. The grown crystals appear to be needles with trigonal axes (c-axes). A sample was a plate cut perpendicular to the c-axis by using a beryllium wire cutter. After being mirror-polished with No. 1500 Al_2O_3 powder, its surfaces were painted with silver paste in order to use as electrodes. The electrical capacitance and dielectric loss tangent were measured with an ac bridge at a frequency of 1 MHz with a weak ac electric field of 15 V/cm, and the existence of the spontaneous polarization was examined by an improved Sawyer-Tower circuit.[8] The temperature of the sample was measured by use of a potentiometer with an alumel-chromel thermocouple directly attached to one of the electrodes.

Two types of high pressure apparatus were used in this work. One is a piston-in-cylinder type with silicone grease as a pressure transmitting fluid[9] and was chiefly used in the high temperature range from 200°C to 260°C, and the other is a simple intensifier type with silicone oil as a pressure transmitting fluid.[10] The pressure transmitting fluid has to be dehydrated by heating up above 100°C in order to prevent the sample from moisture.

§3. Experimental Results and Discussion

3.1 *Pressure and temperature dependence of relative permittivity*

(i) *II-III phase transition*

Before the dielectric measurement is done for the II-III phase transition with pressure, we first have to raise the temperature of the sample along a dot-dashed line shown in Fig. 5 from room temperature to 215~255°C in order to put the sample in the state of phase IV into the state of phase II through the phase III. The solid lines in Fig. 1 show the pressure dependence of the relative permittivity along

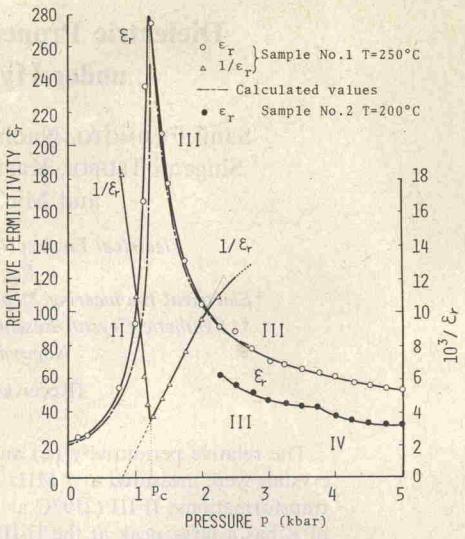

Fig. 1. The pressure dependence of the relative permittivity along the c-axis (ε_r) at constant temperatures.

the c-axis (ε_r) at constant temperatures. The value of ε_r has a large peak at the transition pressure (p_c). The reciprocal relative permittivity ($1/\varepsilon_r$) at pressures above p_c (in the phase III) increases linearly with pressure near p_c, i.e., $1/\varepsilon_r$ obeys the Curie-Weiss law on pressure.

According to the phenomenological theory for the first order antiferroelectrics under hydrostatic pressure,[11] the relative permittivity (ε_r) is given by the following equations

$$1/\varepsilon_r\varepsilon_0=(u+gp+f)/2 \qquad (1)$$

in the paraelectric phase, and

$$1/\varepsilon_r\varepsilon_0=3f-2(u+gp)+(4h/3)\times\{1+\sqrt{1+3(f-u-gp)/(2h)}\} \qquad (2)$$

in the antiferroelectric phase, where ε_0 is the vacuum permittivity, u the coefficient of $P_a^2+P_b^2$ (P_a, P_b: spontaneous polarizations of sublattices), g the coefficient of the electrostrictive term, f the coefficient of P_aP_b, and h the constant associated with the coefficients of the fourth and sixth power of P_a or P_b.

The dot-dashed line in Fig. 1 shows the calculated ε_r by putting $u=-1.89\times10^9$ m/F, $g=1.85\times10^9$ m/F·kbar, $f=3.92\times10^8$ m/F and $h=6.04\times10^7$ m/F* into eqs. (1) and (2). The calculated value is in good agreement with the measured value, so the phases II and III seem

* The detailed method for the determination of these coefficients has been described in ref. 11.

to be antiferroelectric and paraelectric, respectively.

(*ii*) *III-IV phase transition*

The small dielectric anomaly on the ε_r vs. p curve for $T=200\,^{\circ}C$ in Fig. 1 corresponds to the III-IV phase transition, and the phase III is at pressures below the transition pressure (p_c) and the phase IV is at pressures above p_c. Except for in the vicinity of the antiferroelectric II-III phase transition, the value of ε_r measured in the phase III and the phase IV decreases with increasing pressure, similarly to other ionic crystals, for example MgO, LiF and NaCl, etc.[12]

Figure 2 shows the temperature dependence of ε_r at temperatures near the IV-III phase transition temperature (T_c) under various pressures. We find the following facts in Fig. 2: (1) the relative permittivity (ε_r) steps up at T_c with increasing temperature and its discontinuous change in ε_r at T_c decreases as the applied pressure increases, (2) the ε_r vs. T curve shifts toward the higher temperature side with an increase of pressure and (3) the phase transition becomes sluggish gradually with increasing pressure.

The decrease of the change in ε_r at T_c with an increase of pressure is explained in terms of the structure of $RbNO_3$ as follows: The NO_3^- ions have two sets of sites in the phase IV, one has a symmetry C_s and the other has a symmetry C_{3v}. After the transformation IV→III, the symmetry of all the sites becomes the same symmetry C_3, leading to the orientational disorder and enhanced rotation of NO_3^- ions.[5] By applying the pressure to $RbNO_3$, the rotation of NO_3^- ions is hindered because of the contraction of the lattice constant. So it is difficult for the state of NO_3^- ions to change into the orientational disorder. Consequently, the change in ε_r at the transition point gets smaller with an increase of pressure.

3.2 *Pressure and temperature dependence of dielectric conductivity*

Figure 3 shows the pressure dependence of the logarithmic dielectric conductivity along the c-axis ($\log_{10}\sigma$) at constant temperatures. The $\log_{10}\sigma$ decreases linearly with pressure in each phase. And the $\log_{10}\sigma$ at $T=236.5\,^{\circ}C$ steps up at the II-III phase transition pressure with increasing pressure, while the $\log_{10}\sigma$ at $T=210\,^{\circ}C$ decreases discontinuously at the III-IV phase transition pressure. These features of $\log_{10}\sigma$ against p at the II-III and III-IV phase transitions coincide qualitatively with those of $\log_{10}\sigma$ against T at the II-III and III-IV phase transitions measured under atmospheric pressure.[5]

Figure 4 shows the $\log_{10}\sigma$ plotted against the reciprocal absolute temperature ($1/T$) at constant pressures. At a pressure of 1 kbar, the $\log_{10}\sigma$ decreases proportionally to $1/T$ in the phase III, and steps down at the III-IV phase transition temperature.

The large increase for $\log_{10}\sigma$ observed in the phase III (against p or T) is considered to be due to the orientational disorder of the NO_3^- ions, since the conductivity of $RbNO_3$ is ionic in nature.[5] Such a consideration is clearly confirmed on experimental results that the change in $\log_{10}\sigma$ at T_c gets smaller by applying

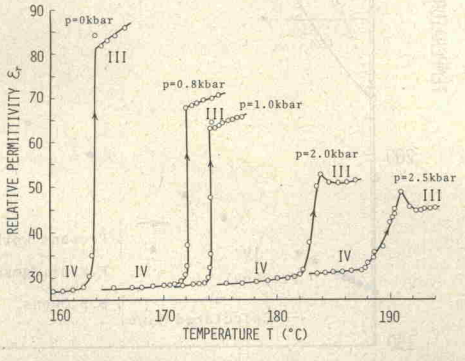

Fig. 2. The temperature dependence of the relative permittivity along the c-axis (ε_r) under various pressures at temperatures near the IV-III transition temperature.

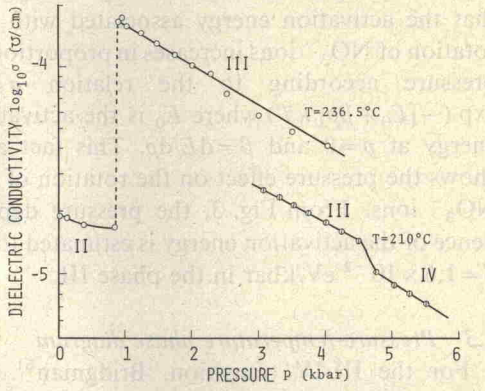

Fig. 3. The pressure dependence of the logarithmic dielectric conductivity at 1 MHz along the c-axis ($\log_{10}\sigma$) at constant temperatures.

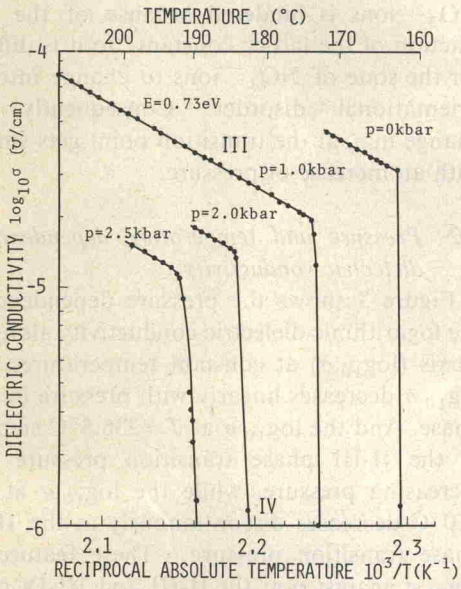

Fig. 4. The reciprocal absolute temperature dependence of the logarithmic dielectric conductivity at 1 MHz along the c-axis ($\log_{10}\sigma$) under various pressures at temperatures near the III-IV transition temperature.

the pressure (see Fig. 4). These phenomena are, as described in §3.1(ii), similar to the change in ε_r at T_c under pressures.

The temperature dependence of σ can be described by the usual relation $\sigma = A \exp(-E/kT)$ where A is a constant, E the activation energy, and k the Boltzmann constant. The slope of $\log_{10}\sigma$ vs. $1/T$ straight line in the phase III (see Fig. 4) gives the activation energy associated with the rotation of NO_3^- ions, and its value is $E=0.73$ eV.

Now, the linear relation between $\log_{10}\sigma$ and p in the phase III as seen in Fig. 3 suggests that the activation energy associated with the rotation of NO_3^- ions increases in proportion to pressure according to the relation $\sigma=A \exp(-[E_0+\beta p]/kT)$ where E_0 is the activation energy at $p=0$ and $\beta=dE/dp$. This fact also shows the pressure effect on the rotation of the NO_3^- ions. From Fig. 3, the pressure dependence of the activation energy is estimated to be $\beta=1.6\times10^{-2}$ eV/kbar in the phase III.

3.3 *Pressure-temperature phase diagram*

For the III-IV transition, Bridgman[6] followed the phase diagram to 6 kbar by means of the volume discontinuity method, and later Rapoport[13] extended the limit of the pressure to 40 kbar by differential thermal analysis. For the II-III transition, Owens[7] reported as follows; (1) there is a triple point (II-III-Liq.) at 315°C and 1.9 kbar and (2) the slope of the transition temperature for the II-III curve is $dT_t/dp=50$ deg/kbar, based on the III-Liquid curve and room pressure thermodynamic and crystallographic data.

Now, we tried to follow the pressure-temperature phase diagram as follows:

(a) The III-IV phase transition points can be determined from the dielectric anomaly of ε_r as seen in Fig. 2, and are shown by closed circles in Fig. 5. Our results are in good agreement with those by Bridgman. Its phase boundary has a straight line with a slope of $dT_c/dp=10$ deg/kbar at lower pressures, but has a slight curvature at higher pressures.

(b) The II-III phase transition points can be determined from peaks of ε_r in ε_r vs. p curves under various temperatures (Fig. 1 is a typical result), and are shown by open circles in Fig. 5. Since the obtained III-II transition temperatures have the fluctuation of ±5°C for each sample, we normalized them to be the average value of

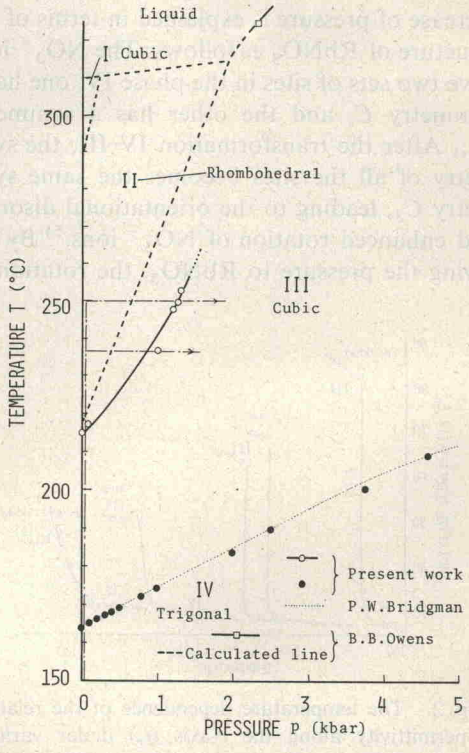

Fig. 5. The pressure-temperature phase diagram of $RbNO_3$.

215°C at atmospheric pressure. The pressure dependence of T_t is estimated to be $dT_t/dp \fallingdotseq 30$ deg/kbar, which is smaller than that calculated by Owens.

§4. Summary

The experimental results are summarized as follows:

(i) The relative permittivity (ε_r) has a peak and dielectric anomaly at the II-III and the III-IV transition pressure, respectively. The behavior of ε_r at the II-III phase transition is explained by the phenomenological theory for the first order antiferroelectric phase transition.

(ii) The dielectric conductivity (σ) steps up at the II-III transition pressure and decreases discontinuously at the III-IV transition pressure. The $\log_{10}\sigma$ decreases in proportion to pressure in each phase, and the σ is described by the relation $\sigma = A \exp(-[E_0 + \beta p]/kT)$.

(iii) At the IV-III transition temperature, the changes in ε_r and σ for the ε_r vs. T and σ vs. T curves get smaller with increasing pressure, and such a behavior of ε_r and σ is understood to be based on the rotation of NO_3^- ions being hindered by pressures.

(iv) The II-III phase boundary could be determined by the dielectric measurement.

In this experiment, no double hysteresis loop was observed in the phase II probably because of the high conductivity and low breakdown electric field strength.

References

1) P. P. Salhotra, E. C. Subbarao and P. Venkateswarlu: Phys. Status solidi **29** (1968) 859.
2) G. A. Samara: J. Phys. Chem. Solids **26** (1965) 121.
3) A. Ya. Dantsiger and E. G. Fesenko: Soviet Physics-Crystallography **8** (1964) 717.
4) P. C. Bury and A. C. McLaren: Phys. Status solidi **31** (1969) 799.
5) P. P. Salhotra, E. C. Subbarao and P. Venkateswarlu: Phys. Status solidi **31** (1969) 233.
6) P. W. Bridgman: Proc. Am. Acad. Arts Sci. **51** (1916) 582.
7) B. B. Owens: J. chem. Phys. **42** (1965) 2259.
8) Y. T. Tsui, P. D. Hinderaker and F. J. McFadden: Rev. sci. Instrum. **39** (1968) 1423.
9) S. Fujimoto, N. Yasuda and M. Koizumi: *Proc. 4th Intern. Conf. on High Pressure, Kyoto* (Physico-chemical Soc. of Japan, 1974) p. 371.
10) K. Gesi, K. Ozawa and Y. Takagi: J. Phys. Soc. Japan **20** (1965) 1773.
11) S. Fujimoto and N. Yasuda: Japan. J. appl. Phys. **15** (1976) 595.
12) S. Mayburg: Phys. Rev. **79** (1950) 375.
13) E. Rapoport: J. Phys. Chem. Solids **27** (1966) 1349.